Improving the Performance of Organic Cathode Materials in Li-ion Batteries through Secondary Interactions

Madison Tuttle

Introduction to Organic Cathode Materials in Li-ion Batteries

Modern society relies heavily on lithium-ion batteries (LIBs) to power every-day devices such as portable laptops, cell phones, and increasingly, electric vehicles.[1,2] The cathode materials employed by traditional LIBs, depend on toxic transition metals, such as Co and Ni, which are unsustainable in both their natural abundance and mining practices. If the dependence of LIBs on unsustainable metals continues, the volatile world metal market will inevitably place a restrictive limitation on battery development.[3,4] In the past decade, rechargeable batteries containing organic-based cathode materials (OCMs) have emerged as an attractive alternative to transition-metal-based cathodes, as many low molecular weight organic molecules have high theoretical capacities and can be synthesized from abundant materials.[5–8] Unfortunately, OCMs often suffer from low conductivity and dissolution into electrolyte, adversely affecting their charging rates and cycle stability,[9–12] therefore motivating the discovery of new design principles to boost OCM performance.

A critical, but often overlooked, difference between OCMs and transition metal oxides cathode is that OCMs lack the covalent interactions between the charge storing units, which are found ubiquitously in transition metal oxide materials.[13,14] Due to the strong overlap of metal-oxide orbitals, transition metal cathodes form conductive electronic networks through which charges can propagate through the bulk of the cathode (Figure 1A). Conversely, the majority of OCMs are composed of individual redox-active units with no mechanism for intermolecular

charge propagation (Figure 1B). As a result, conductive carbon doping (as high as 50%-90%)[5–8,15] or the addition of conjugated linkers between charge storage units is often required for acceptable cycling performance.[16,17] For example, despite the fast electron transfer kinetics of individual TEMPO ((2,2,6,6-tetramethylpiperidin-1-yl)oxyl),[18] TEMPO polymers such as PTMA are found to be electrically insulating due to the inadequate charge propagation through the bulk of the material (Figure 1B).[17,19] Thus, OCMs based on polymeric TEMPO require high percentages of conductive carbon additives in order to achieve adequate conductivity and cycling performance.[20–22] The incorporation of crosslinkers between polymer chains has also been shown to improve the cyclability,[16,17] but at the cost of reducing the already low specific capacity of polymeric TEMPO to an impractical value.

Thus, we wish to formulate design principles with emphasis on the charge transfer between organic charge storage units in order to address performance issues of OCMs, such as low conductivity and capacity retention. We propose that electronic interactions between charge-storage units may provide a mechanism for charge propagation, mimicking that found in metal oxide materials. Consequently, we hypothesize that the deliberate inclusion of electronic interactions such as

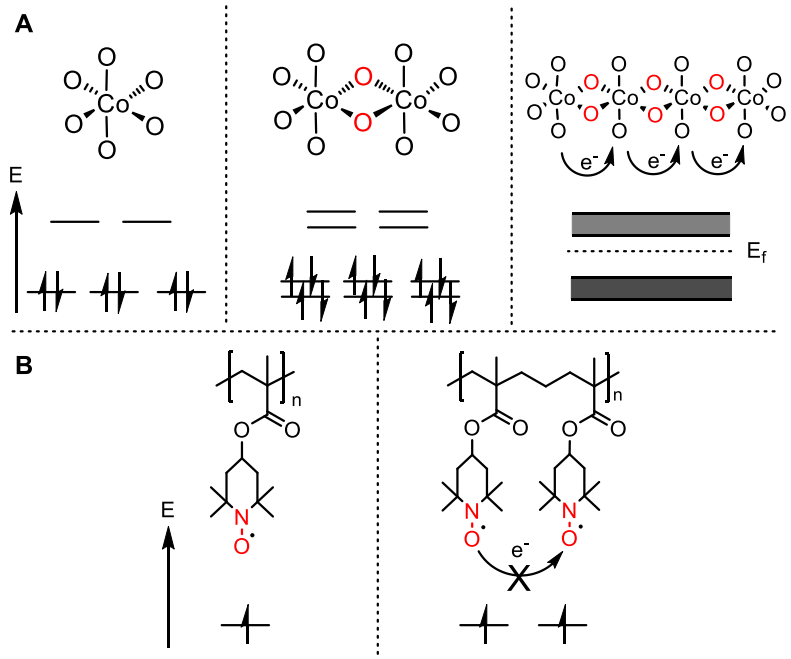

Figure 1. Frontier orbitals resulting from the interaction or lack thereof between charge storing units in (A) cobalt (IV) oxide and (B) poly-TEMPO. Labeled in red are key atoms responsible for (A) bridging charge storing units or (B) storing charge.

hydrogen bonding (Aim 1) and electrostatic interactions (Aim 2) could improve the cycling stability and rate capability of OCMs.

Aim 1: Hydrogen Bonding

Hydrogen bonding (H-bonding) is ubiquitous in nature and often utilized to create strong, stable supramolecular constructs, i.e. complementary base pairs in DNA.[23] This stabilization effect extends generally to molecules in solution, but more importantly to molecules in the solid state. In the solid state, H-bonding promotes the alignment, or ordering, of molecules due to the directionality of H-bonds, which exhibit a preference toward linear donor-acceptor angles between 160-170°.[24] The directional alignment of molecules due to H-bonding can greatly affect intermolecular electron delocalization (Figure 2), with greater alignment associated with enhanced electrical conductivity, as exhibited by several H-bonded organic semiconductors.[25–31] Notably, a recently reported tetrathiafulvalene semiconductor with a highly ordered solid-state structure resulting from H-bonding exhibits an electrical conductivity of 0.29 Ω cm, the highest electrical conductivity reported for pure organic, single-phase semiconductors.[32] Thus, we hypothesize that the incorporation of H-bond donor/acceptor interactions into charge-storage units should increase the conductivity, and in turn, the rate capability of OCMs by facilitating molecular ordering.

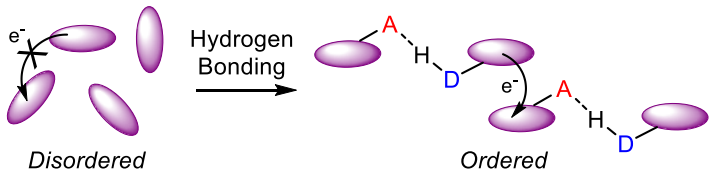

Figure 2. Illustration of the effect of hydrogen bonding on molecular ordering and electrical conductivity. The purple ellipsoids represent generic organic charge-storage units. A represents a generic hydrogen bond acceptor, and D represents a generic hydrogen bond donor.

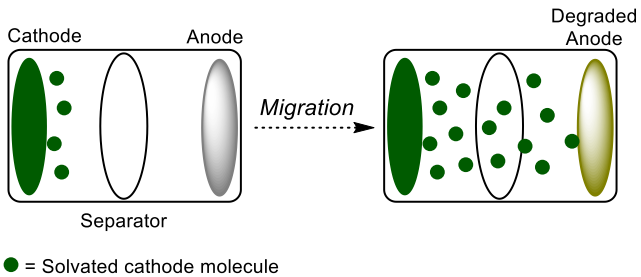

Figure 3. Illustration of self-discharge in a Li-ion coin cell.

Additionally, H-bonding has a significant impact on solubility, an issue that has traditionally plagued OCMs.[6,33–35] For example, quinones are attractive building blocks for OCMs due to their reversible redox behavior, high energy densities, and modular chemical structures. However, the practical use of quinone-based OCMs is restricted by their tendency toward self-discharge,[6,36,37] a process by which a material dissolves into the battery electrolyte, migrates through the cathode/anode separator, and chemically reacts with the anode (Figure 3). In general, H-bonding decreases solubility of organic molecules in nonpolar solvents (i.e., ether-based battery solvents) due to the polar nature of H-bonds and the poor H-bond accepting/donating ability of nonpolar solvents.[38] Therefore, H-bonding can be utilized to prevent self-discharge in OCMs. In fact, the recent work of Vlad *et al*. shows that the incorporation of $-NH_2$ groups onto a quinone scaffold can decrease the solubility in battery electrolytes and allow for a moderate increase in capacity retention.[39] Based on this work, we are optimistic that H-bonding between charge-storage units can increase the cycle stability of OCMs by decreasing the solubility in battery electrolytes, but we would like to explore the generalizability of this phenomenon.

Scheme 1. OCM design to probe the efficacy of H-bond donor/acceptor interactions in battery performance. Theoretical capacities are denoted underneath.

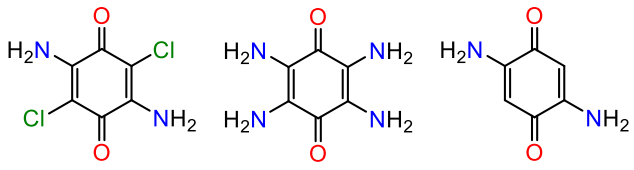

To assess the effect of H-bonding on the rate capability and cycle stability of OCMs, we selected a set of four benzoamines (Scheme 1) to test as cathodes in Li-ion coin-type cells, including 2,5-diamino-3,6-dichloroquinone (**Cl_2DAQ**),[40] 2,3,5,6-tetraaminoquinone (**TAQ**),[41] and the original 2,5-diaminoquinone (**DAQ**)[39,40] tested by Vlad *et al*. These benzoquinones include amino substituents as the H-bond donors and carbonyls and chloro substituents as the H-bond

acceptors. When designing this basis set, we considered two key aspects: (1) the number of H-bond donors/acceptors, and (2) the proximity of H-bond donors/acceptors.

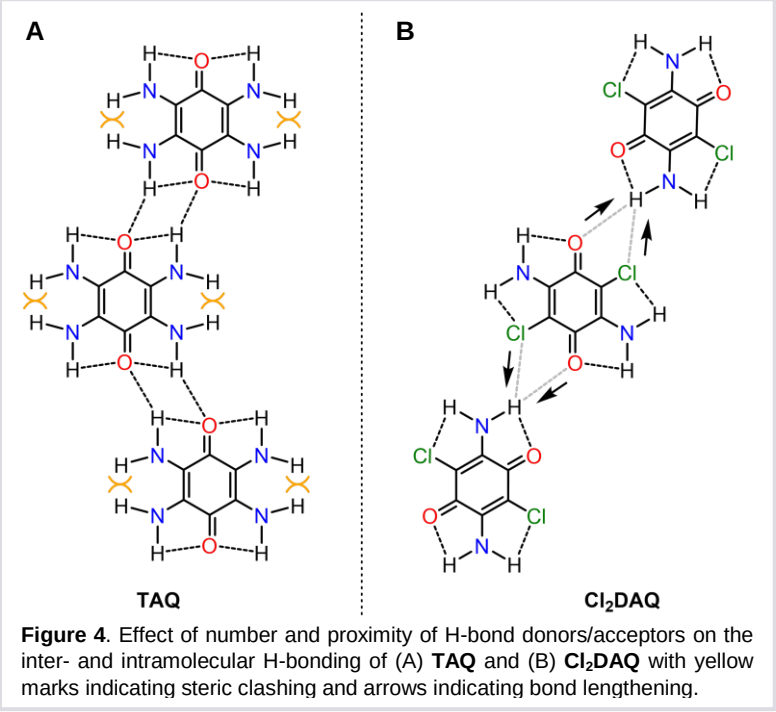

Figure 4. Effect of number and proximity of H-bond donors/acceptors on the inter- and intramolecular H-bonding of (A) **TAQ** and (B) **Cl₂DAQ** with yellow marks indicating steric clashing and arrows indicating bond lengthening.

First, we hypothesize that a greater ratio of H-bond donors to acceptors will positively correlate with battery performance such that **TAQ** (1:2 ratio of H-bond donors to acceptors) > **DAQ** (1:1 ratio of H-bond donors to acceptors) > **Cl₂DAQ** (2:1 ratio of H-bond donors to acceptors). This is because the incorporation of more H-bond donors (**TAQ**) increases the probability of intermolecular and intramolecular H-bonding, which together will decrease the solubility further than intermolecular H-bonding alone (Figure 4). Furthermore, we envisioned that intramolecular H-bonding would also decrease the flexibility of the H-bond donors such that the solid-state system is more ordered (Figure 4A), which could boost conductivity. On the other hand, we expect a greater ratio of H-bond acceptors to donors (**Cl₂DAQ**) will be detrimental to battery performance because the increased number of acceptors will likely compete for H-bonding with intermolecular donors such that two acceptors are bound to one donor (Figure 4B), which may decrease the overall order within the solid state system and lead to poor battery performance.

Next, we thought that closer H-bond donor/acceptor proximity would negatively correlate with battery performance such that **DAQ** > **TAQ** > **Cl₂DAQ**. In this case, we believe that the

proximity of the H-bond donors in **TAQ** may decrease intramolecular H-bonding due to steric repulsion (Figure 4A), which will decrease the molecular ordering in the solid state and adversely affect battery performance. Similarly, we believe that the proximity of the H-bond acceptors in **Cl_2DAQ** will negatively affect intermolecular H-bonding due to deviation from the preferred donor-acceptor angles of 160-170° (Figure 4B), which causes an increase in H-bond length.[24] This lengthening not only weakens the intermolecular H-bond but also distances two molecules from one another, making charge transfer more difficult.

With this in mind, we will first probe the H-bond strength of the basis set in solution as this could have strong implications for self-discharge and battery performance. We will investigate the thermodynamic parameters, (i.e., equilibrium constants, enthalpy, and entropy) of molecular aggregation resulting from H-bonding with isothermal titration calorimetry as well as NMR.[42–46] By isothermal titration calorimetry (ITC), we will measure temperature differences over time as the concentration of **TAQ**, **DAQ**, or **Cl_2DAQ** is increased. The change in heat per mole of injectant will be plotted as a function of concentration to obtain thermodynamic parameters of H-bonding. ^{1}H, ^{13}C, and ^{15}N NMR will be used to monitor the change in chemical shift as a function of concentration and temperature to obtain similar thermodynamic parameters. A comparison of the results from both ITC and NMR experiments will afford an accurate description of the strength of intermolecular H-bonding in **TAQ**, **DAQ**, and **Cl_2DAQ**.

We then wish to obtain structural evidence of how H-bonding affects the solid-state structures of **Cl_2DAQ** and **TAQ** (crystal structures have already been reported for **DAQ**) by either single-crystal or powder X-ray diffractometry. Metric parameters of H-bonding (length and angle) and molecular packing will provide support for the relative performance of these compounds as OCMs.

Next, we plan to study the redox abilities of these compounds with solution phase CV. As all three compounds in our basis sets are quinones, we expect to see two reversible redox couples for each compound. Additionally, we note that under our electrochemical conditions, we should not observe proton reduction to H_2. Organic compounds that participate in proton reduction usually act as a hydritic proton source, producing H_2 in protic solvents or in the presence of acid.[47–49] Thus, as our compounds do not contain hydritic protons and both solution phase and battery solvents are aprotic, we do not expect proton reduction to affect battery performance.

We will then assess the performance of **Cl_2DAQ**, **TAQ**, and **DAQ** as cathodes in Li-ion coin cells. To this end, we will examine the redox behavior in the solid state with solid-state CV, the conductivity and redox kinetics with PEIS, and the overall performance with galvanostatic charging and discharging experiments. According to our rationale above, we expect that **TAQ** will have the lowest internal resistance due to increased ordering in the solid state, and **Cl_2DAQ** will have the highest. Similarly, we expect that batteries made with **TAQ** cathodes will exhibit the highest capacity retention over several cycles as well as the fastest cycling rate compared to either **DAQ** or **Cl_2DAQ**.

Finally, to evaluate the cathode material at different stages of redox, we can perform *in situ* powder X-ray diffraction (PXRD) experiments, as well as post-mortem analysis using FT-IR spectroscopy. We will study the structural changes of these compounds after redox events with *in situ* PXRD, as in the work by Vlad *et al.*[39] Using a specialized PXRD sample holder, we can imitate the environment of a Li-ion coin cell and detect changes in the powder diffraction pattern of the cathode after a redox event has occurred. Similarly, we will monitor the vibrational frequency of the C-O bonds at different stages of redox by obtaining air-free IR data of the cathode material. With these techniques, we can establish whether the structural changes associated with

reduction/oxidation are in fact completely reversible, and whether chemical degradation of the cathode occurs during cycling.

Together, the results of our proposed experiments will provide insight into the ability of H-bonding to impact overall OCM performance, particularly with regard to conductivity and capacity retention. With this knowledge, we can determine whether H-bonding should be considered an important factor when designing new OCMs. Additionally, if H-bonding is beneficial for OCM performance, this work may provide specific H-bond parameters to consider in further OCM design and optimization.

Aim 2: Electrostatic Interactions

Zwitterions are often called inner salts, as they possess both positively and negatively charged regions with a net zero charge. Due to their intrinsic ionic nature, zwitterions can form intermolecular ion-ion interactions with other zwitterions that are spatially inverted or stacked (Figure 5A). Thus, these interactions can result in a network of directionally aligned ion pairs,[50–53] similar to that formed by H-bonding interactions. As stated previously, H-bonding enhances conductivity through the directional alignment of molecules.[25–31] We envision a similar enhancement occurring due to the directional alignment of zwitterions in the solid state (Figure 5B), thus facilitating charge propagation without the need for direct orbital interactions. Notably, a conjugated polymer zwitterion utilized as an electron transport interlayer in an organic

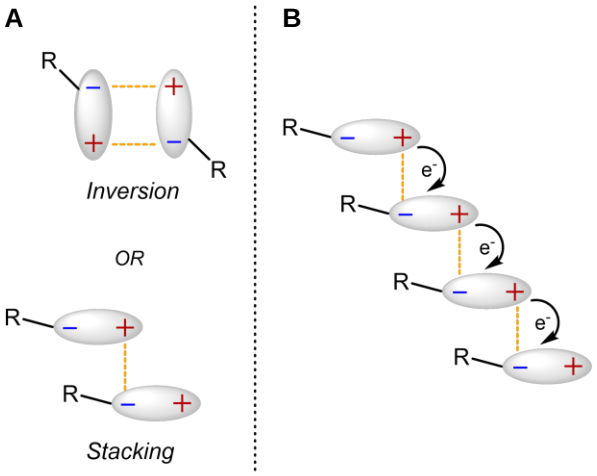

Figure 5. Illustration of ion-ion pairing (orange bonds) between (A) inverted and stacked zwitterions (gray ellipsoids) and (B) zwitterions in a charge transfer network.

photovoltaic device was found to directionally align on a metal surface due to electrostatic interactions, resulting in increased efficiency.[50] Based on this work, we are optimistic that directional alignment due to electrostatic interactions can facilitate charge propagation through a zwitterionic material. Therefore, we hypothesize that zwitterionic OCMs should exhibit increased conductivity and rate capability due to electrostatic molecular alignment.

Furthermore, electrostatic interactions directly influence the solubility of chemical compounds in solution, which can be exploited to prevent self-discharge in OCMs. In general, electrostatic interactions are stronger in nonpolar solvents, i.e., typical battery solvents, resulting in the significantly decreased solubility of ionic compounds.[54] However, as battery solvents often contain a polar carbonate counterpart, it is necessary to consider the strength of electrostatic interactions in polar solvents. Several studies on supramolecular recognition and self-assembly demonstrate that electrostatic interactions between organic ion pairs in polar solvents such as water are entropy driven, such that ion pairing occurs due to the increase in entropy resulting from the release of solvent molecules upon pairing.[38,55–61] A similar effect is observed in a study by Jan Ravoo *et al.* in which the ion pairing of two zwitterionic guests is required for host-guest complexation to occur in polar solvents.[53] Additionally, Endo, *et al.* report a zwitterionic polymer that is insoluble in most common solvents, including dimethylformamide and water, due to purely electrostatic interactions (no H-bonding is present).[62] Thus, we hypothesize that zwitterionic OCMs should exhibit decreased self-discharge and increased capacity retention due to electrostatic interactions between zwitterionic charge-storage units.

To investigate the effect of electrostatic interactions on the rate capability and capacity retention of OCMs, we chose a set of three tetraphenylhexaazaanthracene (TPHA) isomers (Scheme 2), originally characterized by Koutentis *et al.*,[63] to test as cathodes in Li-ion coin-type

cells. These isomers include zwitterionic 1,3,7,9-tetraphenylhexaazaanthracene (**TPHA-1**), non-charge-separated 1,3,7,8-tetraphenylhexaazaanthracene (**TPHA-2**), and zwitterionic 1,3,7,8-tetraphenylhexaazaanthracene (**TPHA-3**). This basis set was designed based on two key aspects: (1) the lack of H-bonding ability in all isomers and (2) the differences in charge distribution between **TPHA-1-3**, resulting from small structural variances.

Scheme 2. OCM design to probe the efficacy of electrostatic interactions in battery performance. Theoretical capacities for one- and two-electron storage are denoted beneath.

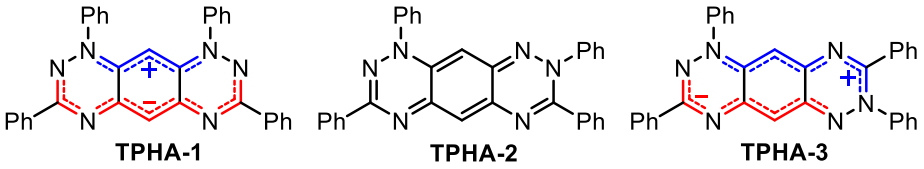

Theor. Cap.
54.6 mAh g^{-1} (1 e^-)
109.3 mAh g^{-1} (2 e^-)

First, we thought it important to select compounds that contained no H-bond donors/acceptors. Many zwitterionic compounds interact with one another via both ion-ion interactions and H-bonding,[50,53,64] which makes investigating the effects of the individual interactions challenging. However, due to the lack of H-bonding ability in the TPHA isomers, we can preclude the assistance of H-bonding in our experiments, especially those regarding battery performance.

Furthermore, the differences in charge distribution of the TPHA basis set are extremely important to our investigations of how electrostatic interactions between zwitterions affect OCM performance. We predict that zwitterions with more orthogonal charge distribution will lead to closer ion-ion interactions and form a more symmetric, ordered solid state system. Considering that conductivity is enhanced with directional alignment, we also predict that orthogonal charge distribution will lead to enhanced conductivity. Additionally, closer ion-ion interactions can help decrease the solubility of the compound. To better visualize how charge distribution might play a role in battery performance, we can look into the crystal packing of these isomers.[63] **TPHA-1** has

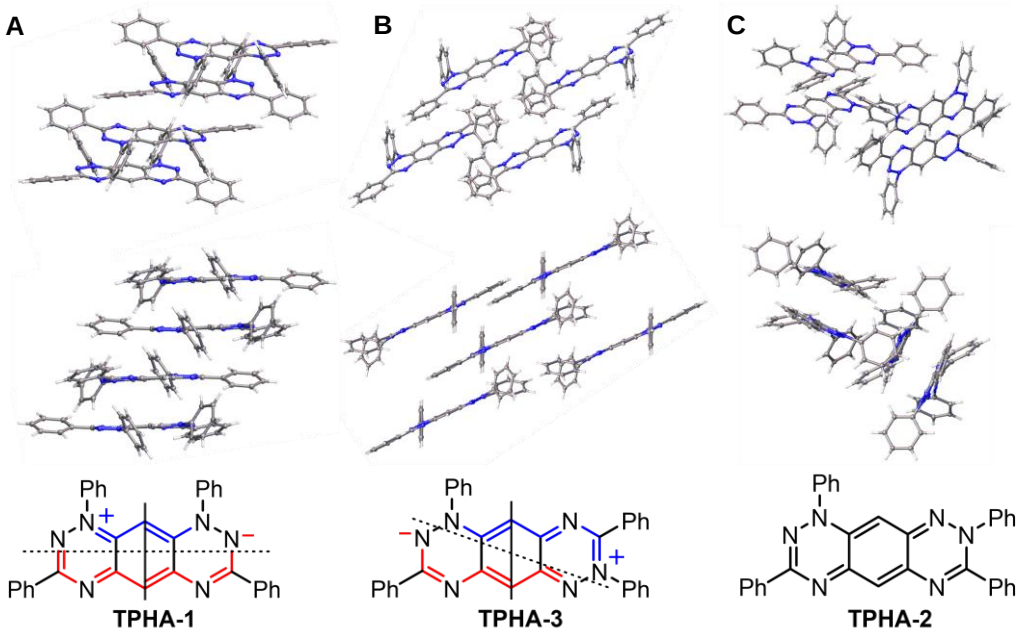

Figure 6. Crystal packing of (A) **TPHA-1**, (B) **TPHA-3**, and (C) **TPHA-2** (top—front view; bottom—side view). Schematic drawings depicting the internal charge separation (dashed line) relative to the center of the ring system (solid line) are shown below.

the most orthogonal charge distribution, and the ion-ion interactions between **THPA-1** zwitterions likely contribute to its symmetric stacking network (Figure 6A). In contrast, the crystal packing of **TPHA-2** and **TPHA-3** are very different from that of **TPHA-1**, due in part to the shift of the phenyl group from the 9-position of the ring system to the 8-position. In particular, the diagonal charge distribution of **TPHA-3** likely leads to elongated ion-ion interactions between **THPA-3** zwitterions, resulting in the less symmetric, brick-layer-type network (Figure 6B). The non-charge-separated **TPHA-2** does not exhibit a network-like structure (Figure 6C), most likely due to a lack of intermolecular ion-ion interactions. Thus, we predict that OCM performance will positively correlate with orthogonal charge distribution such that **TPHA-1**>**TPHA-3**>**THPA-2**.

Similarly, we considered the charge partitioning of the charge-separated π-system in the zwitterionic isomers **TPHA-1** and **TPHA-3**. Calculations of **TPHA-1** and **TPHA-3** suggest that **TPHA-1** partitions into 6π positive biscyanine and 10π biscyanine whereas **TPHA-3** partitions into two oppositely charged 8π cyanines.[63,65] Initially, we thought that the unequal charge

partitioning in **TPHA-1** would result in a decrease in intermolecular electrostatic interactions. However, although the π-system of **TPHA-1** is less symmetric than **TPHA-3** in terms of charge partitioning, the calculated the dipole moments of **TPHA-1-3** reveal that **TPHA-1** actually has a larger dipole moment (6.53 D) compared to both **TPHA-3** (6.09 D) and **TPHA-2** (5.47 D).[63] Based on these data, we believe that the larger dipole moment in **TPHA-1** may lead to stronger intermolecular electrostatic interactions. Indeed, DSC measurements of **TPHA-1-3** show the melting points to be 379 °C, 285 °C, and 290 °C, respectively.[63] Taken together, these qualitative experiments demonstrate that **THPA-1** has stronger intermolecular interactions than either **TPHA-2** or **TPHA-3**. Thus, we predict that **TPHA-1** will perform better as an OCM than **TPHA-2** or **TPHA-3** based on the increased strength of electrostatic interactions.

With these predictions in mind, we will first assess the strength of intermolecular electrostatic interactions of **TPHA-1-3** in solution as this could have strong implications for self-discharge and battery performance. As in Aim 1, we can utilize isothermal titration calorimetry as well as dilution and variable temperature ^{1}H, ^{13}C, and ^{15}N NMR to obtain thermodynamic parameters, i.e., equilibrium constants, enthalpy, and entropy, related to molecular aggregation resulting from electrostatic interactions. These parameters will give us some insight into how the TPHA basis set will behave in battery electrolyte, which is directly related to battery performance.

We then plan to study the redox abilities of these compounds with solution phase CV as well as UV-vis- and EPR-coupled spectroelectrochemistry. The CV of **TPHA-2** and **TPHA-3** has yet to be reported. On the other hand, **TPHA-1** is reported to have two reversible reductions, but only the first is both chemically and electrochemically reversible.[65,66] By comparison of the CVs of **TPHA-1-3**, we can correlate any observed differences to solid state CV as well as battery performance. Additionally, we can further study the electrochemical reactions observed in CV

with UV-vis spectroelectrochemical measurements. **TPHA-1-3** exhibit lowest energy transitions with absorption maxima at 589 nm, 624 nm, and 687 nm, respectively.[63] By spectroelectrochemical measurements, we can monitor changes in these maxima during an electrochemical reaction, which can provide information on how reduction/oxidation affects the lowest energy transition as well as which transitions relate to chemically and electrochemically reversible species. In the same manner, we can monitor changes in the EPR spectrum during an electrochemical reaction, which may provide useful structural information based on observed nuclear-spin couplings.

We will then assess the performance of **TPHA-1**, **TPHA-2**, and **TPHA-3** as cathodes in Li-ion coin cells. To this end, we will examine the redox behavior in the solid state with solid state CV, the conductivity and redox kinetics with PEIS, and the overall performance with galvanostatic charging and discharging experiments. According to our rationale above, we expect that **TPHA-1** will have the lowest internal resistance due to increased ordering in the solid state, and **TPHA-2** will have the highest. Similarly, we expect that batteries made with **TPHA-1** cathodes will exhibit the highest capacity retention over several cycles as well as the fastest cycling rate compared to either **TPHA-2** or **TPHA-3**.

Finally, to evaluate the cathode material at different stages of redox, we will perform *in situ* PXRD experiments as in Aim 1. As the cathode is reduced, a loss of zwitterionic pairing may affect the crystallinity of the material. As a result, the PXRD spectrum may become broader. Additionally, by indexing the PXRD peaks, it is possible to obtain the space group and packing.[67] If loss of pairing negatively affects crystallinity, a lower symmetry space group and packing will be obtained. Similarly, we can perform post-mortem analysis of the cathode material utilizing *ex-situ* ^{15}N and ^{13}C solid-state NMR to determine how discharging/charging affects the chemical

shifts of these nuclei, as described in the work by Loh, *et al*.[15] With these techniques, we can establish whether the structural changes associated with reduction/oxidation are in fact completely reversible, and whether chemical degradation of the cathode occurs during cycling.

Together, the results of our proposed experiments will provide insight into the ability of electrostatic interactions to impact overall OCM performance, particularly with regard to conductivity and capacity retention. With this knowledge, we can determine whether electrostatic interactions should be considered an important factor when designing new OCMs. Additionally, if electrostatic interactions are beneficial for OCM performance, the design and optimization of organic zwitterions for OCMs may be considered a new direction of study in the field of organic batteries.

References

(1) Armand, M.; Tarascon, J.-M. Building Better Batteries. *Nature* **2008**, *451*, 652.

(2) Goodenough, J. B.; Kim, Y. Challenges for Rechargeable Batteries. *J. Power Sources* **2011**, *196*, 6688.

(3) Di Lecce, D.; Verrelli, R.; Hassoun, J. Lithium-Ion Batteries for Sustainable Energy Storage: Recent Advances towards New Cell Configurations. *Green Chem.* **2017**, *19*, 3442.

(4) Gaines, L. Lithium-Ion Battery Recycling Processes: Research towards a Sustainable Course. *Sustain. Mater. Technol.* **2018**, *17*, e00068.

(5) Bhosale, M. E.; Chae, S.; Kim, J. M.; Choi, J.-Y. Organic Small Molecules and Polymers as an Electrode Material for Rechargeable Lithium Ion Batteries. *J. Mater. Chem. A* **2018**, *6*, 19885.

(6) Häupler, B.; Wild, A.; Schubert, U. S. Carbonyls: Powerful Organic Materials for Secondary Batteries. *Adv. Energy Mater.* **2015**, *5*, 1402034.

(7) Larcher, D.; Tarascon, J. M. Towards Greener and More Sustainable Batteries for Electrical Energy Storage. *Nat. Chem.* **2015**, *7*, 19.

(8) Muench, S.; Wild, A.; Friebe, C.; Häupler, B.; Janoschka, T.; Schubert, U. S. Polymer-Based Organic Batteries. *Chem. Rev.* **2016**, *116*, 9438.

(9) Morita, Y.; Nishida, S.; Murata, T.; Moriguchi, M.; Ueda, A.; Satoh, M.; Arifuku, K.;

Sato, K.; Takui, T. Organic Tailored Batteries Materials Using Stable Open-Shell Molecules with Degenerate Frontier Orbitals. *Nat. Mater.* **2011**, *10*, 947.

(10) Kim, D. J.; Hermann, K. R.; Prokofjevs, A.; Otley, M. T.; Pezzato, C.; Owczarek, M.; Stoddart, J. F. Redox-Active Macrocycles for Organic Rechargeable Batteries. *J. Am. Chem. Soc.* **2017**, *139*, 6635.

(11) Chen, D.; Avestro, A.-J.; Chen, Z.; Sun, J.; Wang, S.; Xiao, M.; Erno, Z.; Algaradah, M. M.; Nassar, M. S.; Amine, K.; et al. A Rigid Naphthalenediimide Triangle for Organic Rechargeable Lithium-Ion Batteries. *Adv. Mater.* **2015**, *27*, 2907.

(12) Luo, Z.; Liu, L.; Zhao, Q.; Li, F.; Chen, J. An Insoluble Benzoquinone-Based Organic Cathode for Use in Rechargeable Lithium-Ion Batteries. *Angew. Chemie Int. Ed.* **2017**, *56*, 12561.

(13) Nitta, N.; Wu, F.; Lee, J. T.; Yushin, G. Li-Ion Battery Materials: Present and Future. *Mater. Today* **2015**, *18*, 252.

(14) Besenhard, J. O. *Handbook of Battery Materials*; Besenhard, J. O., Ed.; Wiley-VCH Verlag GmbH: Weinheim, Germany, 2007.

(15) Peng, C.; Ning, G.-H.; Su, J.; Zhong, G.; Tang, W.; Tian, B.; Su, C.; Yu, D.; Zu, L.; Yang, J.; et al. Reversible Multi-Electron Redox Chemistry of π-Conjugated N-Containing Heteroaromatic Molecule-Based Organic Cathodes. *Nat. Energy* **2017**, *2*, 17074.

(16) Aydin, M.; Esat, B. A Polythiophene Derivative Bearing Two Electroactive Groups per Monomer as a Cathode Material for Rechargeable Batteries. *J. Solid State Electrochem.* **2015**, *19*, 2275.

(17) Kim, J.-K.; Kim, Y.; Park, S.; Ko, H.; Kim, Y. Encapsulation of Organic Active Materials in Carbon Nanotubes for Application to High-Electrochemical-Performance Sodium Batteries. *Energy Environ. Sci.* **2015**, *9*, 1264.

(18) Suga, T.; Pu, Y. J.; Oyaizu, K.; Nishide, H. Electron-Transfer Kinetics of Nitroxide Radicals as an Electrode-Active Material. *Bull. Chem. Soc. Jpn.* **2004**, *77*, 2203.

(19) Zhang, Y.; Park, A.; Cintora, A.; McMillan, S. R.; Harmon, N. J.; Moehle, A.; Flatté, M. E.; Fuchs, G. D.; Ober, C. K. Impact of the Synthesis Method on the Solid-State Charge Transport of Radical Polymers. *J. Mater. Chem. C* **2017**, *6*, 111.

(20) Bugnon, L.; Morton, C. J. H.; Novak, P.; Vetter, J.; Nesvadba, P. Synthesis of Poly(4-Methyacryloyloxy-TEMPO) via Group-Transfer Polymerization and Its Evaluation in Organic Radical Battery. *Chem. Mater.* **2007**, *19*, 2910.

(21) Oyaizu, K.; Ando, Y.; Konishi, H.; Nishide, H. Nernstian Adsorbate-like Bulk Layer of Organic Radical Polymers for High-Density Charge Storage Purposes. *J. Am. Chem. Soc.* **2008**, *130*, 14459.

(22) Kim, J.-K.; Cheruvally, G.; Ahn, J.-H.; Seo, Y.-G.; Choi, D. S.; Lee, S.-H.; Song, C. E. Organic Radical Battery with PTMA Cathode: Effect of PTMA Content on Electrochemical Properties. *J. Ind. Eng. Chem.* **2008**, *14*, 371.

(23) Watson, J. D.; Crick, F. H. C. Molecular Structure of Nucleic Acids: A Structure for Deoxyribose Nucleic Acid. *Nature* **1953**, *171*, 737.

(24) Steiner, T. The Hydrogen Bond in the Solid State. *Angew. Chemie Int. Ed.* **2002**, *41*, 48.

(25) Neilands, O.; Tilika, V.; Sudmale, I.; Grigorjeva, I.; Edzina, A.; Fonavs, E.; Muzikante, I. Dioxo- and Aminooxopyrimidotetrathiafulvalenes: π-Electron Donors for Design of Conducting Materials Containing Intramolecular Hydrogen Bonds of Nucleic Acid Base Pair Type. *Adv. Mater. Opt. Electron.* **1997**, *7*, 39.

(26) Ueda, A.; Yamada, S.; Isono, T.; Kamo, H.; Nakao, A.; Kumai, R.; Nakao, H.; Murakami, Y.; Yamamoto, K.; Nishio, Y.; et al. Hydrogen-Bond-Dynamics-Based Switching of Conductivity and Magnetism: A Phase Transition Caused by Deuterium and Electron Transfer in a Hydrogen-Bonded Purely Organic Conductor Crystal. *J. Am. Chem. Soc.* **2014**, *136*, 12184.

(27) Gonz Alez-Rodrı´guezrodrı´guez, D.; Schenning, A. P. H. J. Hydrogen-Bonded Supramolecular π-Functional Materials †. *Chem. Mater* **2011**, *23*, 310.

(28) Yoshioka, M.; Saigo, K.; Ogura, T.; Kobayashi, Y.; Hashizume, D. Hydrogen-Bonding-Assisted Self-Doping in Tetrathiafulvalene (TTF) Conductor. *J. Am. Chem. Soc.* **2009**, *131*, 9995.

(29) Murata, T.; Morita, Y.; Fukui, K.; Sato, K.; Shiomi, D.; Takui, T.; Maesato, M.; Yamochi, H.; Saito, G.; Nakasuji, K. A Purely Organic Molecular Metal Based on a Hydrogen-Bonded Charge-Transfer Complex: Crystal Structure and Electronic Properties of TTF-Imidazole-p-Chloranil. *Angew. Chemie Int. Ed.* **2004**, *43*, 6343.

(30) El-Ghayoury, A.; Mézière, C.; Simonov, S.; Zorina, L.; Cobián, M.; Canadell, E.; Rovira, C.; Náfrádi, B.; Sipos, B.; Forró, L.; et al. A Neutral Zwitterionic Molecular Solid. *Chem. - A Eur. J.* **2010**, *16*, 14051.

(31) Balodis, K.; Khasanov, S.; Chong, C.; Maesato, M.; Yamochi, H.; Saito, G.; Neilands, O. Single Component Betainic Conductor: Pyrimido-Fused TTF Derivatives Having Ethylenedioxy Group. *Synth. Met.* **2003**, *133–134*, 353.

(32) Isono, T.; Kamo, H.; Ueda, A.; Takahashi, K.; Nakao, A.; Kumai, R.; Nakao, H.; Kobayashi, K.; Murakami, Y.; Mori, H. Hydrogen Bond-Promoted Metallic State in a Purely Organic Single-Component Conductor under Pressure. *Nat. Commun.* **2013**, *4*, 1344.

(33) Zhao, Q.; Guo, C.; Lu, Y.; Liu, L.; Liang, J.; Chen, J. Rechargeable Lithium Batteries with Electrodes of Small Organic Carbonyl Salts and Advanced Electrolytes. *Ind. Eng. Chem. Res.* **2016**, *55*, 5795.

(34) Zhao, Q.; Zhu, Z.; Chen, J. Molecular Engineering with Organic Carbonyl Electrode Materials for Advanced Stationary and Redox Flow Rechargeable Batteries. *Adv. Mater.* **2017**, *29*, 1607007.

(35) Liang, Y.; Tao, Z.; Chen, J. Organic Electrode Materials for Rechargeable Lithium Batteries. *Adv. Energy Mater.* **2012**, *2*, 742.

(36) Xie, J.; Zhang, Q. Recent Progress in Rechargeable Lithium Batteries with Organic Materials as Promising Electrodes. *J. Mater. Chem. A* **2016**, *4*, 7091.

(37) Yokoji, T.; Kameyama, Y.; Maruyama, N.; Matsubara, H. High-Capacity Organic Cathode Active Materials of 2,2′-Bis-p-Benzoquinone Derivatives for Rechargeable Batteries. *J. Mater. Chem. A* **2016**, *4*, 5457.

(38) Hunter, C. A. Quantifying Intermolecular Interactions: Guidelines for the Molecular Recognition Toolbox. *Angew. Chemie Int. Ed.* **2004**, *43*, 5310.

(39) Sieuw, L.; Jouhara, A.; Quarez, É.; Auger, C.; Gohy, J. F.; Poizot, P.; Vlad, A. A H-Bond Stabilized Quinone Electrode Material for Li-Organic Batteries: The Strength of Weak Bonds. *Chem. Sci.* **2019**, *10*, 418.

(40) Inbasekaran, M.; Strom, R. A Convenient Synthesis of 2,5-Diamino-1,4-Benzenediol. *Org. Prep. Proced. Int.* **1991**, *23*, 447.

(41) Manivannan, R.; Ciattini, S.; Chelazzi, L.; Elango, K. P. Benzoquinone-Imidazole Hybrids as Selective Colorimetric Sensors for Cyanide in Aqueous, Solid and Gas Phases. *RSC Adv.* **2015**, *5*, 87341.

(42) Holdgate, G. A.; Ward, W. H. J. Measurements of Binding Thermodynamics in Drug Discovery. *Drug Discov. Today* **2005**, *10*, 1543.

(43) Sharrow, S. D.; Edmonds, K. A.; Goodman, M. A.; Novotny, M. V; Stone, M. J. Thermodynamic Consequences of Disrupting a Water-Mediated Hydrogen Bond Network in a Protein:Pheromone Complex. *Protein Sci.* **2005**, *14*, 249.

(44) Turnbull, W. B.; Daranas, A. H. On the Value of c: Can Low Affinity Systems Be Studied by Isothermal Titration Calorimetry? *J. Am. Chem. Soc.* **2003**, *125*, 14859.

(45) Schofield, M. H.; Morton, J. G.; Koshland, S. R.; Joe, C. L.; Londergan, C. H.; Stolla, M. C. NMR Determination of Hydrogen Bond Thermodynamics in a Simple Diamide: A Physical Chemistry Experiment. *J. Chem. Educ.* **2015**, *92*, 1086.

(46) Sundin, A.; Račkauskaitė, D.; Orentas, E.; Butkus, E.; Bergquist, K.-E.; Wärnmark, K.; Shi, Q. A Remarkably Complex Supramolecular Hydrogen-Bonded Decameric Capsule Formed from an Enantiopure C 2 -Symmetric Monomer by Solvent-Responsive Aggregation. *J. Am. Chem. Soc.* **2015**, *137*, 10536.

(47) Sevov, C. S.; Hendriks, K. H.; Sanford, M. S. Low-Potential Pyridinium Anolyte for Aqueous Redox Flow Batteries. *J. Phys. Chem. C* **2017**, *121*, 24376.

(48) Lim, C. H.; Holder, A. M.; Hynes, J. T.; Musgrave, C. B. Reduction of CO2 to Methanol Catalyzed by a Biomimetic Organo-Hydride Produced from Pyridine. *J. Am. Chem. Soc.* **2014**, *136*, 16081.

(49) Barton Cole, E.; Lakkaraju, P. S.; Rampulla, D. M.; Morris, A. J.; Abelev, E.; Bocarsly, A. B. Using a One-Electron Shuttle for the Multielectron Reduction of CO 2 to Methanol: Kinetic, Mechanistic, and Structural Insights. *J. Am. Chem. Soc.* **2010**, *132*, 11539.

(50) Liu, Y.; Duzhko, V. V; Page, Z. A.; Emrick, T.; Russell, T. P. Conjugated Polymer

Zwitterions: Efficient Interlayer Materials in Organic Electronics. *Acc. Chem. Res.* **2016**, *49*, 2478.

(51) Pham, V. H.; Dang, T. T.; Hur, S. H.; Kim, E. J.; Chung, J. S. Highly Conductive Poly(Methyl Methacrylate) (PMMA)-Reduced Graphene Oxide Composite Prepared by Self-Assembly of PMMA Latex and Graphene Oxide through Electrostatic Interaction. *ACS Appl. Mater. Interfaces* **2012**, *4*, 2630.

(52) Stockton W. B.; Rubner M. F. Molecular-Level Processing of Conjugated Polymers .4. Layer-by-Layer Manipulation of Polyaniline via Hydrogen-Bonding Interactions. *Macromolecules* **1997**, *30*, 2717.

(53) Voskuhl, J.; Fenske, T.; Stuart, M. C. A.; Wibbeling, B.; Schmuck, C.; Ravoo, B. J. Molecular Recognition of Vesicles: Host-Guest Interactions Combined with Specific Dimerization of Zwitterions. *Chem. - A Eur. J.* **2010**, *16*, 8300.

(54) Janz, G. J.; Tomkins, R. P. T.; Ambrose, J. *Nonaqueous Electrolytes Handbook. Volume I*; Academic Press, 1972.

(55) Schneider, H. J.; Schiestel, T.; Zimmermann, P. Host-Guest Supramolecular Chemistry. 34. The Incremental Approach to Noncovalent Interactions: Coulomb and van Der Waals Effects in Organic Ion Pairs. *J. Am. Chem. Soc.* **2005**, *114*, 7698.

(56) Berger, M.; Schmidtchen, F. P. The Binding of Sulfate Anions by Guanidinium Receptors Is Entropy-Driven. *Angew. Chemie Int. Ed.* **1998**, *37*, 2694.

(57) Grawe, T.; Schrader, T.; Gurrath, M.; Kraft, A.; Osterod, F. Self-Organization of Spheroidal Molecular Assemblies in Polar Solvents. *Org. Lett.* **2002**, *2*, 29.

(58) Corbellini, F.; Di Costanzo, L.; Crego-Calama, M.; Geremia, S.; Reinhoudt, D. N. Guest Encapsulation in a Water-Soluble Molecular Capsule Based on Ionic Interactions. *J. Am. Chem. Soc.* **2003**, *125*, 9946.

(59) Corbellini, F.; Knegtel, R. M. A.; Grootenhuis, P. D. J.; Crego-Calama, M.; Reinhoudt, D. N. Water-Soluble Molecular Capsules: Self-Assembly and Binding Properties. *Chem. - A Eur. J.* **2005**, *11*, 298.

(60) Corbellini, F.; Fiammengo, R.; Timmerman, P.; Crego-Calama, M.; Versluis, K.; Heck, A. J. R.; Luyten, I.; Reinhoudt, D. N. Guest Encapsulation and Self-Assembly of Molecular Capsules in Polar Solvents via Multiple Ionic Interactions. *J. Am. Chem. Soc.* **2002**, *124*, 6569.

(61) Fiammengo, R.; Timmerman, P.; De Jong, F.; Reinhoudt, D. N. Highly Stable Cage-like Complexes by Self-Assembly of Tetracationic Zn(II) Porphyrinates and Tetrasulfonatocalix[4]Arenes in Polar Solvents. *Chem. Commun.* **2000**, *0*, 2313.

(62) Yamauchi, A.; Matsumoto, K.; Endo, T. Synthesis of Polymers Having Zwitterionic Structure via the Radical Polymerization of 4-Vinylphenyl Isothiocyanate/Cyclic Amidine Adduct. *J. Polym. Sci. Part A Polym. Chem.* **2018**, *56*, 2303.

(63) Constantinides, C. P.; Zissimou, G. A.; Berezin, A. A.; Ioannou, T. A.; Manoli, M.; Tsokkou, D.; Theodorou, E.; Hayes, S. C.; Koutentis, P. A.

Tetraphenylhexaazaanthracenes: 16π Weakly Antiaromatic Species with Singlet Ground States. *Org. Lett.* **2015**, *17*, 4026.

(64) Tortonda, F. R.; Pascual-Ahuir, J.-L.; Silla, E.; Tuñón, I.; Ramírez, F. J. Aminoacid Zwitterions in Solution: Geometric, Energetic, and Vibrational Analysis Using Density Functional Theory-Continuum Model Calculations. *J. Chem. Phys.* **1998**, *109*, 592.

(65) Hutchison, K.; Srdanov, G.; Hicks, R.; Yu, H.; Wudl, F.; Strassner, T.; Nendel, M.; Houk, K. N. Tetraphenylhexaazaanthracene: A Case for Dominance of Cyanine Ion Stabilization Overwhelming 16π Antiaromaticity. *J. Am. Chem. Soc.* **2002**, *120*, 2989.

(66) Zissimou, G. A.; Constantinides, C. P.; Manoli, M.; Pieridou, G. K.; Hayes, S. C.; Koutentis, P. A. Oxidation of Tetraphenylhexaazaanthracene: Accessing a Scissor Dimer of a 16π Biscyanine. *Org. Lett* **2016**, *18*, 15.

(67) Lekin, K.; Winter, S. M.; Downie, L. E.; Bao, X.; Tse, J. S.; Desgreniers, S.; Secco, R. A.; Dube, P. A.; Oakley, R. T. Hysteretic Spin Crossover between a Bisdithiazolyl Radical and Its Hypervalent σ-Dimer. *J. Am. Chem. Soc.* **2010**, *132*, 16212.